New Journal of Physics
The open-access journal for physics

Universality in the merging dynamics of parametric active contours: a study in MRI based lung segmentation

Amit K Chattopadhyay[1,3], **Nilanjan Ray**[2] **and Scott T Acton**[2]

[1] Mathematics Institute, University of Warwick, Gibbet Hill Road, Coventry CV4 7AL, UK

[2] Department of Electrical and Computer Engineering, Thornton Hall, 351 McCormick Road, PO Box 400743, Charlottesville, VA 22904-4743, USA

E-mail: amit@maths.warwick.ac.uk, nray@virginia.edu and acton@virginia.edu

New Journal of Physics **7** (2005) 148
Received 31 January 2005
Published 21 June 2005
Online at http://www.njp.org/
doi:10.1088/1367-2630/7/1/148

Abstract. Measurement of lung ventilation is one of the most reliable techniques in diagnosing pulmonary diseases. The time-consuming and bias-prone traditional methods using hyperpolarized H^3He and ^1H magnetic resonance imageries have recently been improved by an automated technique based on 'multiple active contour evolution'. This method involves a simultaneous evolution of multiple initial conditions, called 'snakes', eventually leading to their 'merging' and is entirely independent of the shapes and sizes of snakes or other parametric details. The objective of this paper is to show, through a theoretical analysis, that the functional dynamics of merging as depicted in the active contour method has a direct analogue in statistical physics and this explains its 'universality'. We show that the multiple active contour method has an universal scaling behaviour akin to that of classical nucleation in two spatial dimensions. We prove our point by comparing the numerically evaluated exponents with an equivalent thermodynamic model.

[3] Author to whom any correspondence should be addressed.

PII: S1367-2630(05)94047-0

Contents

1. Introduction

Ventilation analysis is an authentic way of diagnosing lung airway diseases. The ratio of the volume of ventilated (functional) portions of lungs to the total lung volume is known as lung ventilation, which is used in validating pulmonary drugs [1, 2]. The process involves two complementary magnetic resonance (MR) imaging modalities, the hyperpolarized helium-3 (H^3He) imagery and the proton (^1H) imagery. Lung functionality, including the volume of ventilated lungs, can be obtained from the former modality while lung anatomic details, including total lung volume, are accessed through the latter [1, 2]. Since manual investigation of the MR imagery to compute lung ventilation is extremely time consuming, an 'active contour' or 'snake' based automated method has been proposed [1]–[4] to compute the total lung volume from proton MR imagery on a two-dimensional (2D) slice-by-slice basis [1]. A snake is defined as a massless 2D thin string (closed or open) that can move on the image domain driven by two types of forces, internal elastic forces and external image forces [5]. Under the influence of these two forces an initial contour (snake) clings to image edges and delineates an object. A snake always gives continuous edges unlike any traditional edge detector (e.g. the Canny method [7]), thereby eliminating any post-processing steps to connect the detected broken edges. These two properties are particularly useful when the object outline is broken and noisy as in most of the ^1H MR imagery. The snake method of finding the object boundary relies on the initial snake placement inside the image. If a small initial snake is placed inside a lung cavity on the MR image, while growing, the snake may be stopped by the associated numerous artifacts and may not capture the actual lung outline [1]. Starting with a larger snake may result in missing the lung cavity completely. A possible solution is to start with multiple non-overlapping small snakes inside the lung cavity and evolve (grow) them until they merge with each other and capture the cavity outline [1]. During such a process, the growing snakes merge with each other into a single contour. This automatic merging of non-overlapping snakes is characterized by certain attributes: (a) during the evolution process no two snakes overlap with each other, (b) every snake stops evolving at the object edge as a single snake does during its course of evolution and (c) growing convex-shaped snakes (e.g., circular or rectangular snakes) inside a convex object recovers the object boundary. Although merging of multiple snakes is experimentally verified in a multitude of cases, a concrete theoretical understanding of this merging snake approach remains a challenge. A principal aim of this paper is to bridge this gap by showing that the underlying principle of multiple snake-merging is governed by a 'universal power law' behaviour which originates from an inherent 'nucleating' structure.

The other focal point of this study is to demonstrate that under suitable design of the force field governing snake evolution, parametric active contours [5] can also achieve automatic merging like geometric contours [6]. Our previous work [1] with the help of segmentation experiments on real MRI data demonstrates that parametric active contours merge with each other while evolving under a force field known as generalized gradient vector flow (GGVF). GGVF is designed by equipping an underlying partial differential equation (PDE) with a Dirichlet boundary condition (5) on the initial snake locations. Segmentation of ^{1}H MRI imagery can also be achieved by using GGVF in conjunction with geometric active contour evolution. However, using multiple parametric snakes for this application is advantageous due to the following reasons. Firstly, if a multiprocessor machine is available, then multiple parametric snake evolution can be performed in parallel very easily as these snakes evolve completely independent of each other from the beginning to the end [1]. Secondly, we can assign different rigidity parameter values (α and β in the snake equation) to different parametric snakes; this strategy often helps to achieve more accurate segmentation. For example, to capture the costophrenic angle (CPA) of lungs, we need a very low value of the rigidity parameters, whereas, in general in other places of the lung cavity, higher values for rigidity parameters help mitigate obstacles due to noise. Thus from a prior knowledge about the position of the CPA, we can provide low rigidity parameter values to the initial snake assigned to delineate CPA. This differential assignment of rigidity parameter values is extremely difficult with a geometric snake, since after two geometric fronts merge, it is hard to keep track of them individually.

2. Generalized active contour method

From a biomedical engineering perspective, the study of the efficacy of the lung cavity delineation method is crucial for robust clinical application. The lung cavity segmentation by merging snake method involves three steps: (a) initially small non-overlapping contours are placed inside the lung cavity, (b) GGVF fields [3] are computed with a Dirichlet boundary condition on the initial circular snakes [1], and (c) all the snakes are evolved simultaneously and independently of each other with the GGVF force field as the external force for the snakes. This automated lung cavity segmentation is attractive for a number of reasons. While other merging snake algorithms, such as the one proposed by McInerney and Terzopolous [8] is computationally non-trivial compared to the original snake evolution algorithm of Kass *et al*'s [5], the merging snake algorithm by Ray *et al* maintains the same computational simplicity of Kass *et al*'s algorithm. Also, based on the position of an initial snake, the rigidity parameters of the snakes can be varied, so that on one hand delicate high curvature features, such as CPAs, can be accurately captured, while on the other hand, snakes can be made sufficiently stiff in order to avoid capturing artifacts. Figures 1–3 show multiple snake initialization, evolution, merging and delineation of lung boundary by the Ray *et al* method.

In order to map the merging snake scenario to statistical thermodynamical systems, we first provide the mathematical background for a parametric active contour or snake. A snake is a curve $\mathbf{C}(s) = (p(s), q(s))$ defined by the parameter $s \in [0, 1]$. The snake is evolved in such a way that it minimizes the energy functional [3]

$$E_s = \int_0^1 \left(\tfrac{1}{2}\{\alpha|\mathbf{C}'(s)|^2 + \beta|\mathbf{C}''(s)|^2\} + E_{\text{ext}}[\mathbf{C}(s)] \right) \mathrm{d}s, \tag{1}$$

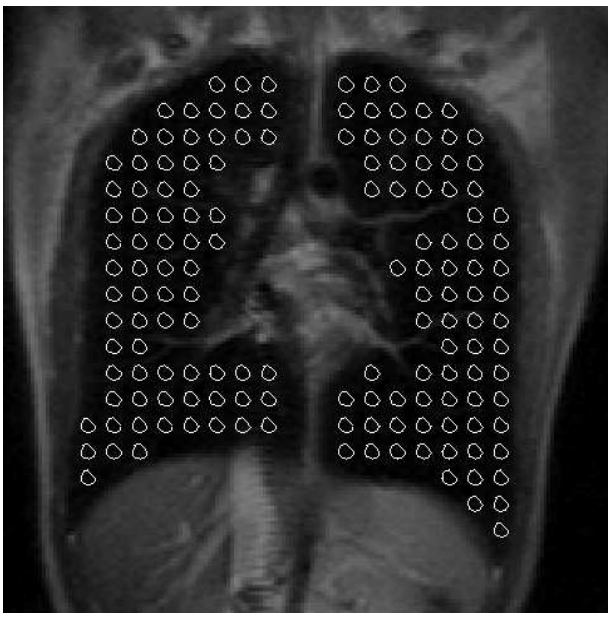

Figure 1. Initial snakes (here circular, although one can use rectangular snakes as well) assigned into a lung cavity on a 2D MRI slice.

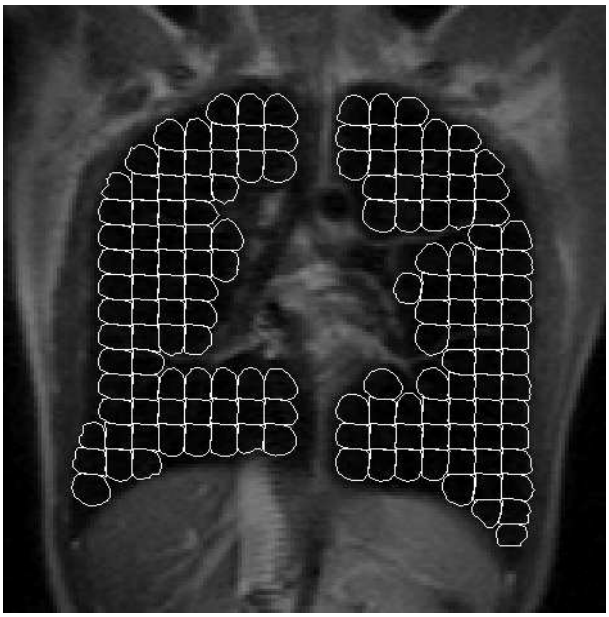

Figure 2. Intermediate snake evolution stage for segmenting the lung cavity shown in figure 1.

where the first two terms give the internal energy of the snake ($\alpha, \beta \geqslant 0$) and E_{ext} represents the external energy added to the system. $\mathbf{C}'$ and $\mathbf{C}''$ are the first and second derivatives of the snake with respect to s. An example of external force for the snake is the gradient force

$$E_{\text{ext}} = -|\nabla I(x, y)|^2, \tag{2}$$

Figure 3. Lung cavity delineation by merging all the snakes after their evolution stopped.

where $I(x, y)$ is the image pixel intensity obtained from 2D lung scans. A remarkable feature of this energy functional is associated with the definition of the external energy E_{ext}. Although the internal energy reminds one of the traditional Gaussian functional form, the overall energy functional nevertheless is devoid of any Ginzburg–Landau feature since the external energy part is not of the ϕ^4 type.

In general, in the presence of an external force $\mathbf{V}(\mathbf{C}(s, t))$ (defined by equation (3)), the time dynamics of such a snake is given by [1, 2]

$$\frac{\partial \mathbf{C}(s,t)}{\partial t} = \alpha \mathbf{C}''(s,t) - \beta \mathbf{C}''''(s,t) + \mathbf{V}(\mathbf{C}(s,t)). \tag{3}$$

The defining force field is the dynamic equivalent of equation (7) and is given by

$$\frac{\partial \mathbf{V}}{\partial t} = g(|\nabla f|)\nabla^2 \mathbf{V} - (1 - g(|\nabla f|))(\mathbf{V} - \nabla f), \tag{4}$$

where $g(\alpha) = \exp(-K\alpha)$ and $f(x, y) = -E_{\text{ext}}(x, y)$. K is the smoothness defining parameter which can be adjusted close to high curvature zones to get a better fit. When n such non-connected snakes, enclosed in regions D, each evolve together in a closed region ∂D, equation (4) is coupled with the Dirichlet condition

$$\begin{aligned} \mathbf{V}(x, y) &= \mathbf{0} \qquad \text{for } (x, y) \in D, \\ \mathbf{V}(x, y) &= \mathbf{n}(x, y) \quad \text{for } (x, y) \in \partial D, \end{aligned} \tag{5}$$

where $\mathbf{n}(x, y)$ is the unit normal at (x, y) on the image domain boundary ∂D. The desired driving force can now be derived by solving the boundary value problem defined in the

vector equation (4) together with equations (5). Numerically, we have used a finite-difference scheme for the discretization in two spatial dimensions. To do so, we define the vector field $\mathbf{V}(x, y) = (u(x, y), w(x, y))$. Equation (4) can now be rewritten as

$$\begin{aligned} \frac{\partial u}{\partial t} &= g(|\nabla f|)\nabla^2 u - (1 - g(|\nabla f|))\left(u - \frac{\partial f}{\partial x}\right), \\ \frac{\partial w}{\partial t} &= g(|\nabla f|)\nabla^2 w - (1 - g(|\nabla f|))\left(w - \frac{\partial f}{\partial y}\right). \end{aligned} \tag{6}$$

One can now map these equations (6) to that of the Navier–Stokes' equations for a viscous incompressible fluid as in [1]. We now solve equations (6) using our self-developed matlab code using a finite-difference algorithm on a variable grid.

The stationary solution of equation (2) corresponds to a snake that minimizes the energy functional. Ray *et al* proposed an external force $V(x, y)$ obtained by solving the following PDE applying Dirichlet boundary condition on the initial snakes [1]:

$$g(|\nabla f|)\nabla^2 \mathbf{V} - (1 - g(|\nabla f|))(\mathbf{V} - \nabla f) = \mathbf{0}, \tag{7}$$

where $g(\alpha) = \exp(-K\alpha)$ and $f(x, y) = -E_{\text{ext}}(x, y)$, K being a tunable parameter controlling the smoothness of the external snake force field. $\mathbf{V}$ is determined from the above equation using Dirichlet boundary conditions. In the following portion, we study the resultant dynamics due to the evolution of a number of such snakes, defined by the above system of forces.

3. Merging dynamics in the active contour method

When multiple snakes are evolved inside the desired closed boundary constrained by specific boundary conditions (that two snakes never cut across each other), the growth algorithm confirms that they all finally merge into a single snake after a finite time. This 'merging of snakes' is basically a topological effect and naively the phenomenology reminds one of 'nucleation' as seen in classical first-order thermodynamic systems [9]. To study this dynamics of merging, we allow a finite number of GGVF snakes, each with a finite starting radius, to evolve in a 2D plane and then numerically evaluate a few measurables—the nucleation time (NT) in units of the total number of iterations, the bounding area (BA) in units of square pixels after nucleation has occurred, the critical radius (CR) in units of pixels at the time of nucleation and also the non-dimensional nucleation rate (NR), all as functions of a non-dimensionalized (i.e. in number of iterations) snake evolution time. The respective quantities are defined as follows—NT is the time required for all the snakes to merge together as a single unit, BA is the sum of the areas of the initial snakes before complete merging and the area under the single snake after merging, CR is the equivalent radius of curvature of the 'nucleated' structure once all the snakes have merged together and NR is the ratio of the number of snakes to the bounding area (BA) before the merging has actually taken place. One should note that by 'complete merging' we refer to the critical phase when all the initial snakes merge together for the first time.

We perform two numerical experiments with merging. In the first experiment, we start with a circular binary image of radius R containing N number of circular snakes, each of radius $r < R$, randomly distributed inside. As described before, the initial snakes are driven by GGVF forces and they maintain a non-overlapping dynamics. In another numerical experiment, we vary the radii of the smaller circles and later also vary their total number (5, 10, 15, 20, 25).

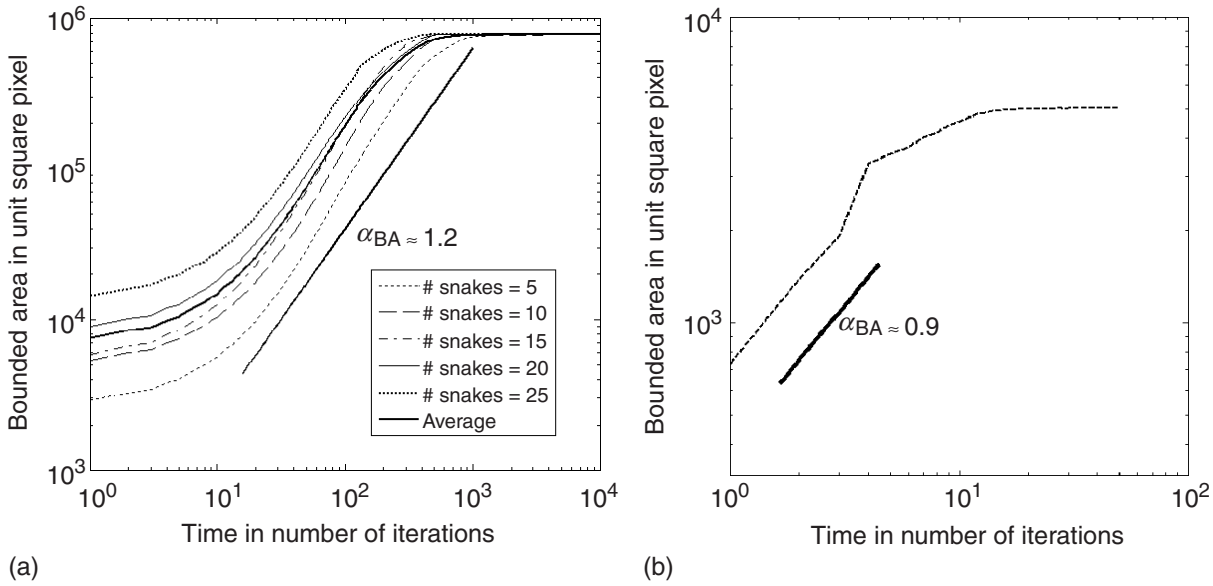

Figure 4. Bounding area (square pixels) versus time (number of iterations) in log–log scale: (a) shows the scaling using our GGVF numerics, (b) gives the equivalent scaling using real lung measurement data.

Both numerics are repeated with varying sizes of the initial domain R. The enclosed figures 3 and 4 show the respective variations of the BA and the CR against non-dimensionalized time in log–log plots. Part (a) of either figure refers to the scaling obtained using GGVF numerical data while the part (b) in each case refers to the lung segmentation data obtained from real life experiments. We could have rescaled the numerical data and plotted both of them on the same graphs, especially since scaling obtained from real data show such remarkable agreement with our numerics. But unfortunately, the scaling zone observed in actual experiments span only about a decade as opposed to our experimental data which through simulations over large snake domains can be stretched up to two decades, essentially retaining nearly the same scaling behaviour. Thus we plot them as separate figures but the punchline here is the nice agreement between real data and GGVF numerics. We will shortly find that the same holds true in our thermodynamic theory as well.

We find that the graphs (figure 4 over two decades in time and figure 5 over one decade in time, after which they saturate) show excellent scaling, with the nonlinear zones referring to the saturation limits in each case. These figures were generated by simulations consuming about 8 computer hours in each case, with a Matlab implementation on a Pentium 4, 2.4 GHz, 1 GB RAM PC. In the figures shown, the bounding image radius is 500 pixel units (i.e., BA of $\pi 500^2$ square pixel units) while the corresponding starting snake radius is 1 pixel unit. Even with such large system sizes we find that the CR saturates within a time decade. To get scaling regimes over larger time periods we would need to employ an inordinately vast amount of computer resources which we do not have at our disposal at the moment. In our simulations, we varied the initial conditions by changing the number of snakes and then studying the resulting dynamics in each case. This is indicated in the legend of the figures (figures 4(a) and 5(a)). The plots show power-law variations of each of the measured quantities with time, i.e. $y \sim x^{\alpha}$ and the two relevant exponents, that of CR and BA, have the values $\alpha_{BA} \approx 1.1$–1.2, $\alpha_{CR} = 0.26$.

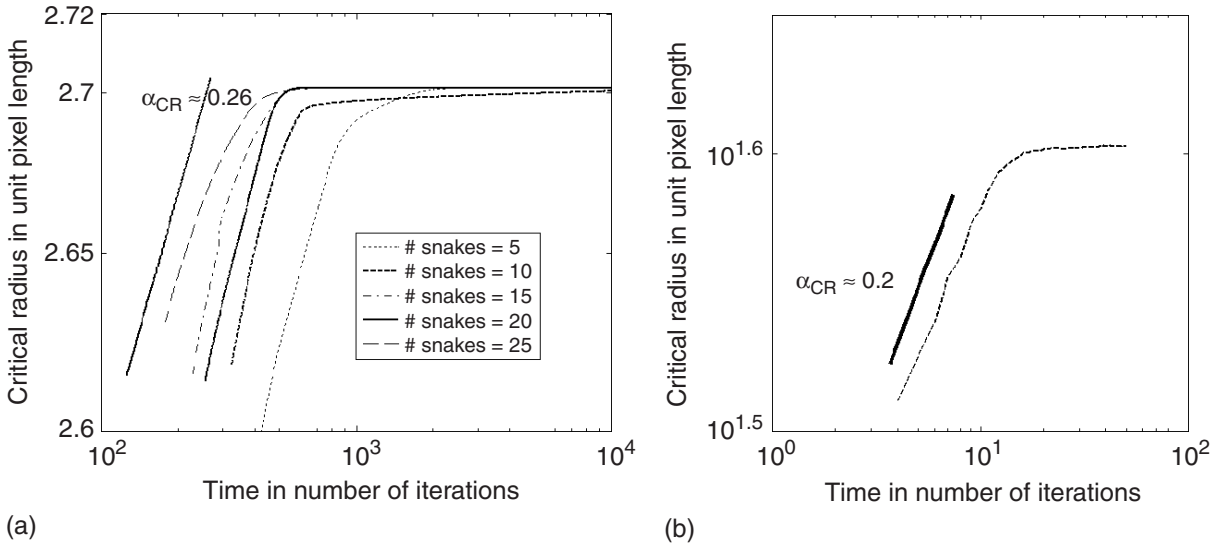

Figure 5. Critical radius (pixels) versus time (number of iterations) in a log–log plot, after complete merging of the snakes: (a) shows the GGVF scaling and (b) comes from the real life data.

We have used multiple combinations of the parameter values but the exponents remain 'universal', that is they invariably follow a power-law statistics with the same exponents independent of the variation in initial conditions or changes in parameter values.

4. Thermodynamic model and discussions

To analyse the results theoretically, we map the merging dynamics scenario to a model of metastable bubbles nucleating under the action of the forces of surface tension. The analysis is based on thermodynamics [9, 12, 13] and our focus will be to probe the 'universal' behaviour observed. Theoretically, this would mean that from our thermodynamic model we want to calculate the critical exponents which are inherent to the active contour dynamics. In what follows, we try to evaluate the time rate of evolution of a system of coalescing snakes before and after all the snakes have completely merged with each other. We map this picture to a model of solutes trying to nucleate in a solution towards a steady, stable state. The thermodynamic problem is thus to find an energetically preferred solution of a system of condensing droplets (or bubbles) such that stability implies a droplet with a minimum critical diameter. All droplets with diameters smaller than this critical value will remain unstable.

Our starting description is that of the diffusive growth of 2D spherical droplets (circles in two spatial dimensions) in a Lifshitz–Slyozov [9]–[11] type of continuum theory. We start with the thermodynamic definition of the work ΔW required to form a nucleus from an aggregate of solute particles

$$\Delta W = \delta(E - T_0 S + P_0 V), \tag{8}$$

where $\delta(E - T_0 S)$ is the increment in the free energy of the system and $\delta(P_0 V)$ is the associated external work done. Minimizing this free energy, one can show [9] that the CR of a nucleating

system is given by

$$R_{\mathrm{CR}} = \frac{\zeta s'}{\mu'(P) - \mu_0'(P)}. \tag{9}$$

Here μ_0' and s' are the chemical potential and molecular surface area of the nucleus, ζ is the surface tension and μ' is the chemical potential of the solute in the solution. To compare with the active contour mechanism, the CR there is defined by the rate of merger of snakes leading to a coarsening feature. If c represents the concentration of the solute in the solution and c_∞ represents the supersaturated concentration, then one can show that

$$\mu' - \mu_0' \simeq T(c - c_\infty)/c_\infty \tag{10}$$

for a solution with temperature T. Combining equations (9) and (10), we get

$$c = c_\infty + \frac{R_{\mathrm{CR}}}{R}(v - c_\infty). \tag{11}$$

As more and more solutes start nucleating, i.e. snakes merge, the solution approaches the critical limit of supersaturation and in the steady state, the CR grows as

$$\frac{\mathrm{d}R(t)}{\mathrm{d}t} = D\left(\frac{\partial c}{\partial r}\right)\Big|_{r=R}, \tag{12}$$

where $c(R)$ represents the spherically symmetric concentration distribution of snakes around a nucleus of radius a, D being the diffusion coefficient. Following the treatment of Lifshitz–Slyozov [9, 10], it can now be easily shown that if $R_{\mathrm{CR}}(0)$ is the CR at the beginning of the merging process ($t = 0$), then for a predominantly diffusive dynamics in a 2D plane, the radius $R(t)$ follows

$$\frac{\mathrm{d}R(t)}{\mathrm{d}t} = \frac{R_{\mathrm{CR}}^2(0)}{R(t)}\left(\frac{1}{R_{\mathrm{CR}}(t)} - \frac{1}{R(t)}\right). \tag{13}$$

We now define the dimensionless quantities $x(t) = \frac{R_{\mathrm{CR}}(t)}{R_{\mathrm{CR}}(0)}$, $u(t) = \frac{R(t)}{R_{\mathrm{CR}}(t)}$ and $\tau = 2\log x(t)$. The last one increases monotonically from 0 to ∞ as the time t increases likewise. Combining equations (12) and (13) in 2D, the dynamics is given by

$$\frac{\mathrm{d}u^2(\tau)}{\mathrm{d}\tau} = \gamma\left(1 - \frac{1}{u}\right) - u^2, \tag{14}$$

where $\gamma = \frac{\mathrm{d}t}{R_{\mathrm{CR}}(0)\mathrm{d}x} > 0$. A linear stability analysis of the above nonlinear equation gives a fixed point at $\gamma_0 = 27/4$. We are interested in the dynamics around an ϵ-neighbourhood of this point γ_0. If $\gamma(\tau) = \frac{27}{4}[1 - \epsilon^2(\tau)]$ ($\epsilon \to 0$ as $\gamma \to \infty$), then near the critical point ($u_0 = (\gamma/2)^{1/3} = 3/2$) the merging snakes follow a dynamics defined by

$$\frac{\mathrm{d}u}{\mathrm{d}\tau} = -2\left(u - \tfrac{3}{2}\right)^2 - \tfrac{3}{4}\epsilon^2. \tag{15}$$

The time variation of the merging nuclei (snakes) is

$$x(t) = \frac{4}{27}\frac{\sqrt{t}}{R_{\mathrm{CR}}(0)}. \tag{16}$$

Thus the BA ($\sim x^2(t)$) of the merging snakes grow at the rate of t which is roughly speaking our numerical estimate (1.1–1.2) also (figure 4(a)). However, the above analysis is only valid before complete merging of the snakes has occurred. In the 'merged' phase, when the resultant asymmetrical structure continues growing finally to coalesce with the bounding image, the system dynamics is modified. To analyse the situation, we start from equation (13). The equation may alternatively be represented as

$$\frac{\mathrm{d}R(t)}{\mathrm{d}t} = \frac{D\delta c(R(t))}{R(t)} \sim \frac{1}{T}\frac{1}{R^2(t)}. \tag{17}$$

T in the above equation is the temperature of the solution in the equivalent thermodynamic problem, which in our case is a measure of the average surface energy E, $E \propto T$, of the system. This follows from the fluctuation–dissipation theorem which is expected to hold good in the active contour dynamics as well. Evidently, in 2D, E goes as $2\pi R/\zeta$. Using these values in the above equation, we see that after complete merging of the snakes has taken place, the effective radius of curvature of the resultant structure grows as $R_{\mathrm{CR}}(t) \sim t^{1/4}$ (figure 5). Once again our numerical result is in commendable harmony with the theory.

5. Conclusions

Our above analysis, both numerical and analytical, clearly suggests that below the apparently simplistic level of the GGVF application, the system dynamics has a more fundamental symmetry. This symmetry comes from the fact that the GGVF method lies in the same universality class as that of a classical nucleation model. There is, however, a notable shortcoming with the GGVF technique, in that it does not allow us the liberty of starting with an initial condition at an arbitrary location. If the snake starts at a position in which a major portion of the initial snake is outside the desired boundary or vice versa, then the snake driven by GGVF will not converge to the actual boundary. Although it can be shown by the Reed–Simon's theorem [14] that a convex set (a circle, say) growing within a larger convex set (a larger circle or rectangle, say) will always merge with the outer boundary under the action of isotropic driving forces, to the best of our knowledge, no such mathematical lemma exists for a convex set growing in a concave set or vice versa. In the present paper, we have theoretically analysed the physical foundation of the GGVF merging technique and have answered the rather puzzling question as to why it works so accurately. In the process, we have shown that the answer lies in the general scaling behaviour of the underlying nucleation dynamics, defined by proper scaling laws. This clearly indicates that an active contour system is in the same universality class as the nucleation model we considered. Our results, in unison with future biomedical applications, are expected to inspire further studies in the understanding of lung-based diseases.

Acknowledgments

AKC gratefully acknowledges partial research funding from the Alexander von Humboldt Foundation during the initial phases of this work. The authors are also grateful to the reviewer of this paper for his/her insightful comments.

References

[1] Ray N, Acton S T, Altes T, de Lange E E and Brookeman J R 2003 *IEEE Trans. Med. Imaging* **22** 189
[2] Ray N, Acton S T and Ley K F 2002 *IEEE Trans. Med. Imaging* **21** 1222
[3] Xu C and Prince J L 1998 *Signal Processing* **71** 131
[4] Xu C and Prince J L 1998 *IEEE Trans. Image Processing* **7** 359
[5] Kass M, Witkin A and Terzopolous D 1987 *Int. J. Comput. Vis.* **1** 321
[6] Osher S and Sethian J A 1988 *J. Comput. Phys.* **79** 1249
[7] Canny J F 1986 *IEEE Trans. Pattern Anal. Machine Intell.* 679
[8] McInerney T and Terzopolous D 2000 *Med. Image Anal.* **4** 73
[9] Gunton J D, San Miguel M and Sahni P S 1983 *Phase Transitions and Critical Phenomena* vol 8, ed C Domb and J L Lebowitz (New York: Academic)
[10] Lifshitz E M and Pitaevskii L P 1981 *Course of Theoretical Physics* vol 10 (Oxford: Butterworth–Heinemann) p 427
[11] Binder K and Stauffer D 1976 *Adv. Phys.* **25** 343
[12] Langer J S 1967 *Ann. Phys.* **41** 108
Langer J S 1969 *Ann. Phys.* **54** 258
[13] Langer J S and Turski L A 1973 *Phys. Rev. A* **8** 3230
Langer J S and Turski L A 1980 *Phys. Rev.* A **22** 2189
[14] Reed M, Simon B and Reed S M 1997 *Methods of Modern Mathematical Physics: Fourier Analysis, Self-adjointness* (New York: Academic)